Life Sciences 227 (2019) 153–165

Contents lists available at ScienceDirect

Life Sciences

journal homepage: www.elsevier.com/locate/lifescie

Targeting non-oncogene ROS pathway by alantolactone in B cell acute lymphoblastic leukemia cells

Xiaoguang Xu[a,1], Lei Huang[b,1], Zilu Zhang[a], Jia Tong[a], Jianqing Mi[a], Yingli Wu[c], Chenli Zhang[b,*], Hua Yan[a,b,**]

[a] Department of Hematology, Rui-Jin Hospital, Shanghai Jiao-Tong University School of Medicine, Shanghai 200025, China
[b] Department of General Practice, Rui-Jin Hospital, Shanghai Jiao-Tong University School of Medicine, Shanghai 200025, China
[c] Hongqiao International Institute of Medicine, Shanghai Tongren Hospital/Faculty of Basic Medicine, Chemical Biology Division of Shanghai Universities E-Institutes, Key Laboratory of Cell Differentiation and Apoptosis of the Chinese Ministry of Education, Shanghai Jiao Tong University School of Medicine, Shanghai 200025, China

ARTICLE INFO

Keywords:
Alantolactone
Apoptosis
Bioinformatics analysis
ROS
DNA damage
B cell acute lymphoblastic leukemia

ABSTRACT

Aims: Alantolactone (ALT) is active component of natural product *Inula helenium* with a lot of pharmacological effects, including anti-tumor effect. The present work aimed to explore the antitumor effect of ALT in B cell acute lymphoblastic leukemia (B-ALL).

Main methods: B-ALL cells were treated with various concentrations of ALT, and then trypan blue assay, Annexin V/PI staining assay, PI staining assay, western blot analysis were employed to measure the effect of ALT on viability, apoptosis and cell cycle in B-ALL cells. In addition, a synthetic bioinformatics method was used to predict the underlying mechanism of antitumor effect of ALT. Then Reactive Oxygen Species (ROS) probe Dihydroethidium (DHE) and 2′,7′-Dichlorodihydrofluorescein diacetate (DCFH-DA) were used to detect accumulation of cellular ROS. Meanwhile, DNA damage was identified by 8-oxoG, p-ATM1987, γ-H2AX and comet assay. In addition, activity of glutathione reductase (GR), thioredoxin reductase (TrxR) and catalase were measured and overexpressed in SEM and RS4;11 cells to study the inhibition on these enzymes. Finally, B-ALL NOD-SCID mouse model was used to test its performance in vivo.

Key findings: ALT showed good antitumor effect in B-ALL in vivo and in vitro through inducing ROS overload, which led to DNA damage. In addition, we found ROS overload caused by ALT was due to its direct inhibition on reductase.

Significance: We found that ALT, a natural product, showing a promising tactic in the therapy of B-ALL by targeting ROS pathway.

1. Introduction

Approximately 80–85% cases of acute lymphoblastic leukemia (ALL) are of B-cell origin. Patients are mainly children; roughly 60% of cases occur in people younger than 20 years [1–3]. Survival in paediatric acute lymphoblastic leukemia has improved to roughly 90% in trials with risk stratification by treatment modification based on patients' pharmacodynamics and pharmacogenomics, improved supportive care, and biological features of leukemic cells [2,4]. However, innovative approaches are still required to further improve survival time while reducing adverse effects. Prognosis still remains poor in infants, adults and patients who have specific genetic alterations including recurring translocations such as t(9;22)(q34;q11) encoding BCR-ABL1, rearrangement of MLL at 11q23 with a variety of partner genes and thus more novel drugs need to be explored to improve their outcomes [5,6].

Reactive oxygen species (ROS) plays an important role in normal cellular processes, but disregulated ROS conduces to the development of various pathological processes, including cancers [7]. Indeed, one of the main features of cancer cells is a persistent prooxidative state which leads to intrinsic oxidative stress when compared with the normal cells, because of their accelerated metabolism [8,9]. In addition, overload of ROS was further aggravated by oncogenic signaling, such as ras, BCR-ABL and c-myc [10,11]. ROS in tumor cells enhances the tumorigenic phenotype and prompts the accumulation of additional mutations that

* Corresponding author.
** Correspondence to: Hua Yan, Department of Hematology, Rui-Jin Hospital, Shanghai Jiao-Tong University School of Medicine, Shanghai 200025, China.
E-mail addresses: zcl10678@rjh.com.cn (C. Zhang), yanhua_candy@163.com (H. Yan).
[1] These authors contributed equally to this work.

https://doi.org/10.1016/j.lfs.2019.04.034
Received 15 January 2019; Received in revised form 14 March 2019; Accepted 15 April 2019
Available online 17 April 2019
0024-3205/

lead to metastatic behavior [12]. Adaptation to this stress phenotype is essential for tumor cells to survive, proliferation, and drug resistance and consequently cancer cells become rely on it that do not generally perform such a vital function in normal cells. However, relatively higher intracellular ROS level in cancer cells renders these cells more assailable to oxidative stress-induced cell death than normal cells and can be exploited for selective cancer therapy [13,14]. And a study conducted by professors Schreiber & Sam W. Lee showed good anti-tumor performance of a ROS inducer piperlongumine, which showed the feasibility and effectivity of triggering cancer cell apoptosis by targeting ROS pathway through increasing cellular ROS level to break redox system balance in cancer cell [15].

In our study, we aimed to find a natural product that both effective in normal B-ALL cells and cells harboring adverse cytogenetic variants like BCR-ABL fusion oncogene and MLL gene rearrangement. And alantolactone has showed good performance. We investigated its anti-tumor effect both in vitro and in vivo in a preclinical B-ALL mice model. And we have demonstrated that alantolactone exert antitumor effect through inducing ROS generation and causing DNA damage, consequently leading to cell cycle arrest and cell apoptosis. In addition, we found B-ALL cell lines with MLL-AF4 and BCR-ABL fusion gene have higher ROS level compared with non-oncogene addiction cell lines Naml6 and thus are more sensitive to oxidative stress-induced cell death, which provided a new insight of targeting those oncogenes without targeting themselves but oncogenes-induced prooxidative state in B-ALL.

2. Materials and methods

2.1. Reagents and cell culture

Alantolactone was purchased from Tauto Biotech Company (Shanghai, China) with purity > 98% and then it was dissolved in dimethyl sulfoxide (DMSO) and stored as aliquots (20 mM) at −20 °C. TXNRD1, PARP-1, caspase-3, caspase-8, caspase-9, p-cdc2 (Tyr15), p-ATM^{1087}, p-ATM, and β-actin antibodies were obtained from Cell Signaling Technology (Massachusetts, USA). Anti-Glutathione Reductase, catalase, γ-H2AX, Cdc2, cdc25c, p-cdc25c (Ser216) antibodies were purchased from Abcam (San Francisco, USA). Cell Counting Kit-8 was purchased from DOJINDO (Kumamoto, Japan). B-ALL cell lines SEM, Naml6, SUP-B15, TOM-1, RS4;11 are gifts from Professor Mi JQ in Blood Research Institute of Rui-jin hospital. SEM, Naml6 and RS4;11 were maintained in RPIM 1640 medium containing 10% fetal bovine serum (FBS), 100 U/ml penicillin and 100 μg/ml streptomycin, at 37 °C, 5% CO_2 incubator. Mononuclear cells isolated from the primary human B cell Acute lymphoblastic leukemia samples by Ficoll-Paque density gradient separation method were cultured in RPIM 1640 medium with 10% Fetal Bovine Serum (FBS) for 1 h, and then the cells were treated with different concentrations of alantolactone.

2.2. Primary MM cells and normal mononuclear cells

Written informed consent was obtained from three B cell acute lymphoblastic leukemia patients and three healthy donors before peripheral blood sample collection, and the project was approved by the Clinical Investigational Reviewing Board of the Shanghai Second Medical University, China. Mononuclear cells were isolated by Ficoll-Paque density gradient separation method and cultured in RPIM 1640 medium with 10% FBS for 1 h, and then the cells were treated with different concentrations of alantolactone.

2.3. Quantification of apoptosis

Apoptosis was determined by Apoptosis Detection Kit containing Annexin V-APC and PI (propidium iodide), which was purchased from ebioscience (USA) and applied according to the manufacturer's instruction. Annexin V-positive and PI-negative cells were regarded as early apoptotic cells, and cells positive for both Annexin V and PI were considered to be undergoing late apoptosis or necrosis [16]. In our study, apoptotic cells are the sum of all the AnnexinV-positive cells.

2.4. Cell cycle assay

The harvested cells were fixed in ice-cold 70% ethanol at −20 °C overnight. Then fixed cells were washed with PBS and then incubated in 100 μl PBS containing RNAase at a concentration of 250 μg/ml for 30 min at 37 °C at dark. After this, another 100ul PBS containing propidium iodide (PI) at a concentration of 100 μg/ml was added and then cells were incubated at dark at 37 °C for 30 min. Next, cells suspension was filtered through a 70 μM Filcon nylon mesh (BD Biosciences). Then samples were analyzed by the BD LSRFortessa Flow cytometer, and final results were analyzed with FlowJo software (V8.6.1).

2.5. Detection of cellular ROS

Cellular ROS level was measured with fluorescence probes DCFH-DA (Beyotime, China) and Dihydroethidium (DHE) (Beyotime, China). Cells were treated with different concentration of alantolactone alone or pretreated with 5 mM NAC for the indicated time, then harvested, washed with PBS and incubated with 10 μM DCFH-DA diluted with 1640 for 30 min at 37 °C. After washed with 1640 medium for three times, DCF fluorescence intensity was analyzed by flow cytometer. Alternatively, cells were incubated with DHE solution at a concentration of 5 μM at 37 °C for 30 min, then washed twice with PBS to wash off extra DHE. Then samples were analyzed by flow cytometer. Data from three independent experiments were quantified.

2.6. Enzymes activity assay

Determination of SOD, thioredoxin reductase (TrxR), glutathione reductase (GR) and catalase activity were practiced as the instruction of the manuals of Catalase Assay Kit (Beyotime, China), Glutathione Reductase Assay Kit (Beyotime, China), Total Superoxide Dismutase Assay Kit with WST-8 (Beyotime, China) and TrxR Assay Kit (Solarbio, China).

2.7. siRNA design and electroporation

SEM cells were electroporated with siRNA as described previously [17]. Oligoribonucleotides have been synthesized by RiboBio (Guangzhou, China). The sequences of the siRNAs targeting MLL-AF4, siMA1 and siMA2, have been described previously [18].

2.8. Animal study

NOD-SCID mice (5–6 w) were injected through tail vein with 1×10^7 cells/0.1 ml of SEM cells. After 7 days when huCD19+ cells could be detected from the peripheral cells of mice, mice were randomized into 2 groups with 8–10 mice per group and treated with (a) vehicle control (30% HS-15, 5% DMSO and 75% normal saline); (b) alantolactone via intraperitoneal injection at a dose of 100 mg/kg every two days for 2 weeks. Death incidents in each group were recorded and weight of mice in two groups was also documented every two days. Kaplan-Meier methods were used to compute the survival analyze. Bone marrow mononuclear cells of mice in two groups were collected on day 28 and labelled with huCD19-APC antibody to measure the tumor burden. Spleens samples were fixed in 4% paraformaldehyde at 4 °C overnight for paraffin embedding and (H&E) staining was performed to observe filtration of SEM cells in spleens. The study was approved by the Shanghai Jiao Tong University School of Medicine Institutional Animal Care & Use Committee.

Table 1
IC50 of alantolactone for 48 h in hematological malignances. Cells were treated with various concentration of alantolactone for 48 h and CCK8 were used to measure inhibition rate and IC50 were calculated with Graphpad7.0. Data are shown as mean ± SD (n = 3).

列1	Cell type	IC50
T-ALL		
1	Jurkat	24.10 ± 0.66
2	Molt-4	18.6 ± 0.18
Myeloma		
3	RPMI-8226	8.2 ± 0.24
4	U266	8.14 ± 0.23
5	LP-1	7.12 ± 0.17
AML		
6	MV4-11	5.2 ± 0.12
7	Molm13	6.4 ± 0.16
8	HL60	5.6 ± 0.19
B-ALL		
9	SEM	3.17 ± 0.11
10	RS4;11	3.52 ± 0.09
11	SUP-B15	4.05 ± 0.12
12	TOM-1	4.15 ± 0.18
13	Naml6	3.89 ± 0.06

2.9. Statistical analysis

All experiments were performed in triplicate. Two-tailed Student's *t*-test was employed for analyzing both in vitro and in vivo data. Mantel-Cox (Log-Rank) test was used for survival analysis. All analysis was performed by Graphpad Prism7.0. A threshold of $P < 0.05$ was considered as statistically significant.

3. Results

3.1. Alantolactone shows extensive antitumor effect in hematological malignances but most sensitive in B cell acute lymphoblastic leukemia

In our study, we have identified alantolactone, a natural product from *Inula helenium*, showed potent antitumor effect in B-ALL cell lines with IC50 for 48 h reaching approximately 3.5 μM. In addition, we have screened the antitumor effect of alantolactone in a variety of hematological neoplasms cell lines, including T cell acute lymphoblastic, myeloma, AML and B cell acute lymphoblastic leukemia and compared sensitivity to it according to their separate IC50 for 48 h. The IC50 of each cell line was listed in Table 1. The results demonstrated that B-ALL cell lines are more sensitive to the alantolactone than other hematological cancer cells. So, we continued our study in B-ALL.

3.2. Cytotoxicity of alantolactone against B cell acute lymphoblastic leukemia cell lines

Here, we found alantolactone induced cell death in a dose-dependent manner, as shown in Fig. 1B. And primary cells from 3 newly diagnosed B cell acute lymphoblastic leukemia patients, including patient 1# diagnosed with MLL-AF4 positive, were treated with different concentrations of alantolactone for 48 h, with results demonstrating that alantolactone was highly toxic to B-ALL primary cells (Fig. 1D). And to test its toxicity to normal cells, peripheral blood mononuclear cells from three healthy donors were treated with alantolactone in different concentration for 24 h and 48 h, and then viability was measured by trypan blue stain assay. Results demonstrated that alantolactone was less toxic to normal cells when compared with tumor cells (Fig. 1C). In conclusion, alantolactone showed potent antitumor effect in B-ALL but little toxicity to normal cells.

3.3. Alantolactone induces cell apoptosis and G2/M arrest in B-ALL

To figure out if alantolactone induced cell apoptosis and cell cycle arrest, Annexin V/PI staining assay for apoptosis and PI staining assay for cell cycle were used. As shown in Fig. 2A, B, alantolactone induced cell apoptosis in a time- and dose-dependent manner. At the same time, apoptosis-associated proteins were semi-quantified by western blot. And an obvious cleavage of PARP-1, capase-3,caspase-8,caspase-9 were observed after treated with different concentration of alantolactone for 12 and 24 h as shown in Fig. 2C, D. In addition, we treated the PBMCs from three B-ALL patients, and got a similar result (Fig. 2E). To investigate the effect of alantolactone on cell cycle, we treated B-ALL cell lines with alantolactone for 12 h in different concentrations and cell cycle was analyzed with flow cytometer. Flow cytometer analysis revealed that treatment with alantolactone for 12 h increased the number of cells in G2/M phase (from 5.66% to 18.51% in 7.5 μM alantolactone group). At the same time, it decreased the number of cells in G0/G1phases (from 56.51% to 32.77% in 7.5 μM alantolactone group), as shown in Fig. 2F, G. These results indicated that alantolactone showed antitumor effect through inducing cell apoptosis and cell cycle arrest.

3.4. The underlying mechanism of alantolactone is predicted with bioinformatics tools

To clarify the antitumor mechanism of the alantolactone, B-ALL cell line SEM were treated with 5 μM alantolactone or DMSO for 24 h, and then subjected to next generation sequencing. Then cluster heat map was drawn with R statistical software according to their expression profile and showed a distinct clustering between alantolactone-treated group and vehicle-treated group, as shown in Fig. 3A. Then differentially expressed genes (DEGs) expression volcano plot presented in Fig. 3B was drawn by R statistical software with a criteria of P value < 0.05 and Fold change (FC) > 2. Enrichment of functions of the DEGs was conducted by metascape platform with the results presented in Fig. 3C. It's anticipated that most enriched biological processes were associated with cell cycle and apoptosis. We noticed that “DNA replication” and “regulation of cellular response to stress” may help to illustrate the underlying mechanism of alantolactone. Furthermore, we performed gene set enrichment analysis (GSEA) and found that cellular stress associated gene set “ROS” was enriched in alantolactone treatment group showed in Fig. 3D and expression of genes in gene set ROS were listed in Fig. 3E. In addition, we uploaded up-regulated and down-regulated genes as a signature to connectivity map, which is a platform containing expression profile of cell samples treated with different drugs, to match with the reserved data to figure out specific drug-treated samples sharing most similar signature with what we uploaded. There was a presupposition that drugs shared similar signature may also share similar mechanism [19,20]. The overall schematic diagram was shown in Fig. 3F. The top 10 drugs were listed in Table 2, and three of them were NF-κB inhibitors which was coincident with the previous reported mechanism of alantolactone [21], and four drugs of them exerted their effect mainly through inducing DNA damage. Then, a hypothesis was formed that alantolactone induced cell apoptosis and cell cycle arrest may through ROS generation and consequently induced oxidized DNA damage.

3.5. Alantolactone exert antitumor effect through generation of cellular reactive oxygen species

With bioinformatics methods, we presumed that the antitumor effect of alantolactone might be associated with ROS generation. In our previous study, we found that SEM, RS4;11 and SUP-B15 were more sensitive to alantolactone than Naml6 in 24 h treatment, as shown in Fig. 4A. And we have detected the background level of ROS in these four cell lines and found background ROS level is higher in SEM, SUP-B15 and RS4;11 than in Naml6 (Fig. 4B), which give us a hind that

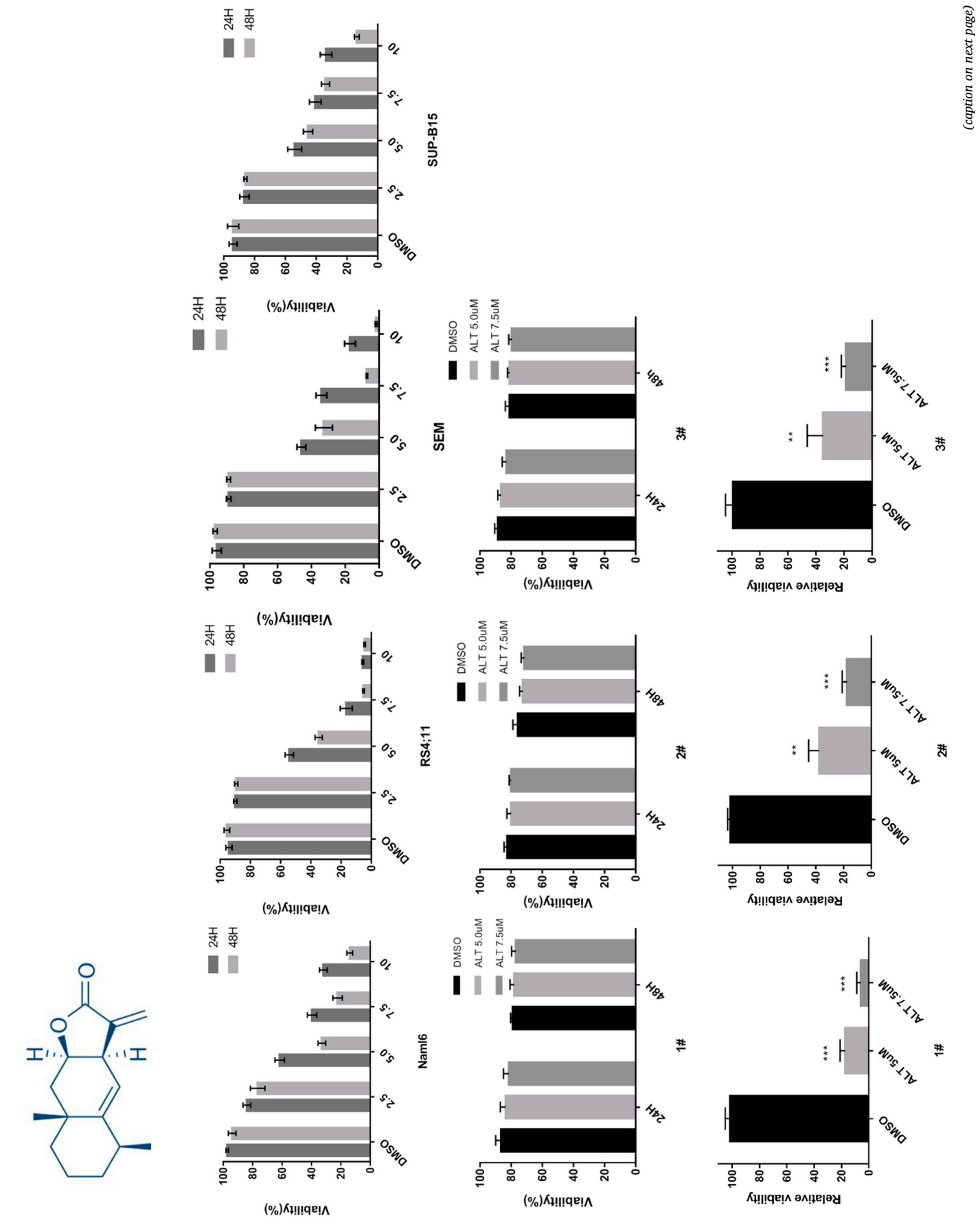

(caption on next page)

Fig. 1. Effect of alantolactone on B-ALL cells cell death. (A) Chemical structure of alantolactone. (B) B-ALL cell lines SEM, Naml6, RS4;11 and SUP-B15 were treated with 2.5 μM, 5.0 μM, 7.5 μM and 10 μM alantolactone or DMSO for 24 h and 48 h and then cell viability was determined by trypan blue stain assay. Each bar represented the mean ± SD of triplicate experiments. (C) PBMCs from three healthy individuals were treated with various alantolactone (2.5, 5.0, 7.5 μM) or DMSO for 24 h and 48 h and viability was determined by trypan blue stain assay. (D) PBMCs from three newly diagnosed B-ALL patients were treated with 5 μM and 7.5 μM alantolactone for 48 h and relatively viability was measured with trypan blue stain assay and then normalized to DMSO treatment group. Data shown are means ± SD (n = 3). Experiments were performed in triplicate ($^{*}P < 0.05$; $^{**}P < 0.01$; $^{***}P < 0.001$).

alantolactone-induced death may be associated with ROS-induced oxidative stress. To further verify the presumed mechanism of alantolactone, we treated B-ALL cell lines SEM and Naml6 with various concentrations of alantolactone for 12 h and then ROS were detected with probes DCFH-DA and DHE. As is revealed in Fig. 4C, D, ROS level of alantolactone-treated SEM cells sharply increased compared with DMSO-treated cells. And we also confirmed this phenomenon in Naml6 cells (Fig. S1). Besides, peripheral blood mononuclear cells from healthy donors were treated with ALT for 20 h and ROS level was detected, with results showing that ALT could not obviously induce ROS generation in healthy cells (Fig. S4). In addition, similar results were obtained with fluorescence microscope in Fig. 4E. And pretreatment with antioxidant NAC could completely reverse alantolactone-induced ROS generation as shown in Fig. 4E, F. It's well established that overload of ROS lead to DNA damage and even cell cycle arrest and cell apoptosis [13]. To further study if the alantolactone-induced cell cycle arrest and apoptosis was caused by overload of ROS. Cell lines were pretreated with 5 mM NAC for 3 h, then subjected to alantolactone treatment to find out if antioxidant could reverse its toxicity. Interestingly, the toxicity of alantolactone was almost fully rescued by NAC pretreatment as it was proved by the reversion of cell viability (Fig. 4G) and apoptosis (Fig. 4H). And we also observed the disappearance of G2/M arrest after pretreatment with NAC (Fig. 4I). In conclusion, these results revealed that the antitumor effect of alantolactone is almost due to the overload of ROS.

3.6. Alantolactone induces extensive DNA damage through ROS overload

It's well established that enhanced ROS levels may lead to oxidative DNA damage, which triggers cell cycle arrest, even programmed cell death if damages exceed repair capacity of cells [13,22]. We presumed that ROS overload induced by alantolactone may result in comprehensive oxidative DNA damage. One of the significant targets of ROS on nucleic acid is the guanine nucleobase and oxidation of guanine generates 8-oxoguanine (8-oxoG) [23,24]. Thus 8-oxoG could be an indicator of ROS-induced DNA damage. To investigate if elevated ROS levels in alantolactone-treated B-ALL cells caused oxidative DNA damage, we first measured total cellular 8-oxoG by immunofluorescent staining with Alexa 488-conjugated avidin, which specifically binds to 8-oxoG. The results showed that treatment with 5 μM alantolactone for 24 h markedly increased intranuclear 8-oxoG level, and treatment with 7.5 μM alantolactone resulted in stronger staining, suggesting a dose-response relationship. While if cells was pretreated with NAC, there almost showed nonoccurrence of 8-oxoG (Fig. 5A, B). In addition, Naml6 and SEM were treated with alantolactone for 12 h and p-ATM^{1987} and γ-H2AX were detected by western blot (WB) to determine the level of DNA damage. Alantolactone could obviously lead the accumulation of p-ATM^{1987} and γ-H2AX and pretreatment with NAC could sharply reduce alantolactone-induced generation of p-ATM1987 and γ-H2AX (Fig. 5C, D).

In addition, we performed the comet assay (single-cell gel electrophoresis), which is a sensitive and simple method in studying DNA damage. The mechanism of it and detailed protocol were described in material and method part. The DNA damage level was measured with olive tail moment. In this experiment, treatment with 5 μM an 7.5 μM alantolactone for 24 h significantly increased the size of comet tail and the number of the cells with a comet tails (Fig. 5E, F), confirming the presence of DNA damage. Pretreatment with 5 mM NAC almost completely prevented the emergence of alantolactone-induced comet tails, which indicated that the DNA lesion was resulted from alantolactone-induced ROS.

3.7. Alantolactone inhibit the activity of several enzymes participating in the elimination of ROS

To further figure out how alantolactone induced ROS generation,

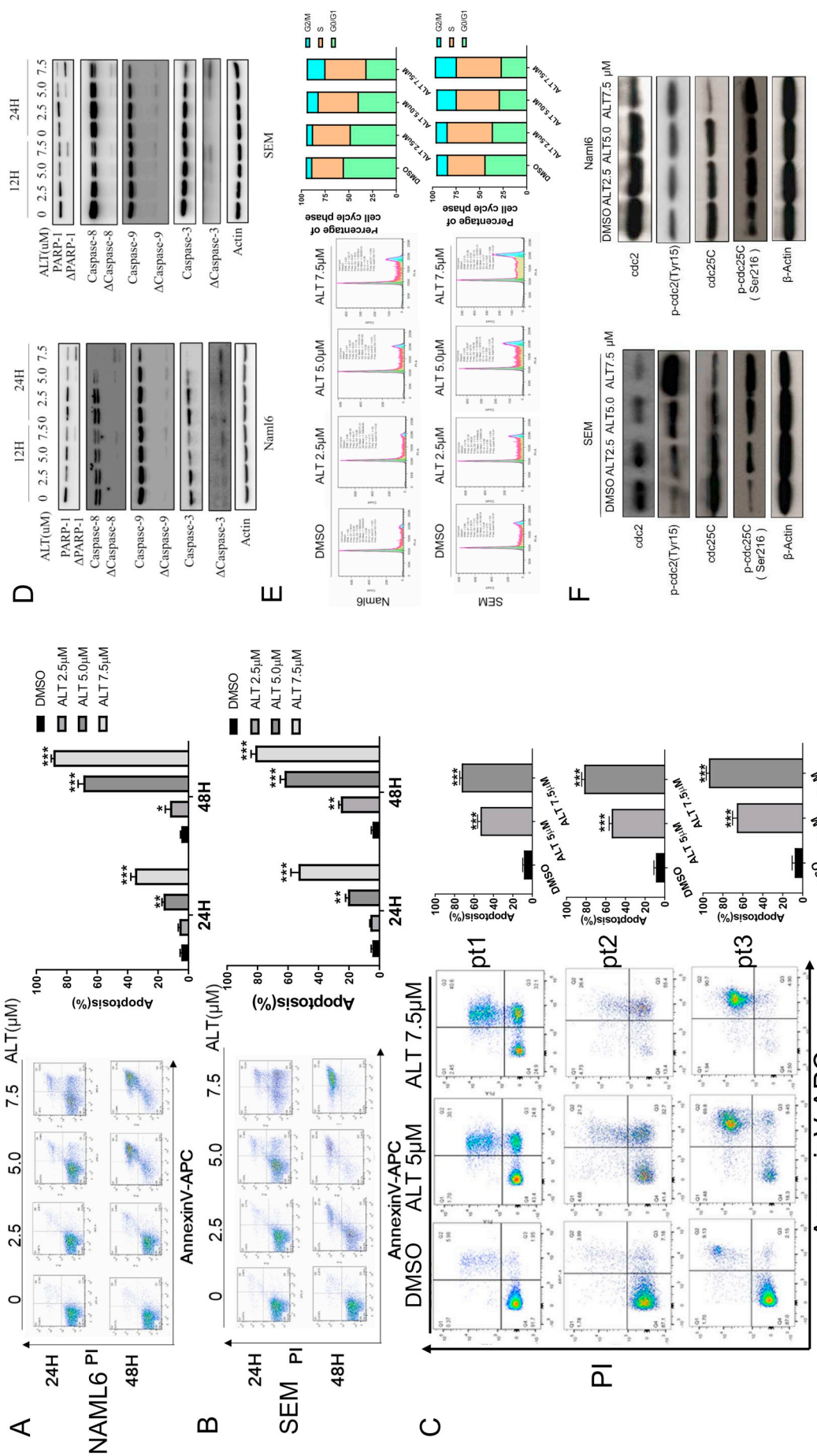

Fig. 2. Alantolactone induced cell apoptosis and cell cycle arrest in B-ALL cells. (A, B) B-ALL cell lines Naml6 and SEM were treated with vehicle solution (0.1% DMSO) and specified concentration of alantolactone (2.5, 5.0, 7.5 μM) in 0.1% DMSO for 24 h and 48 h, and cell apoptosis was determined by Annexin V/PI staining assay. Experiments were performed in triplicate (*$P < 0.05$; **$P < 0.01$; ***$P < 0.001$). (C) PBMCs from three B-ALL patients were treated with alantolactone for 48 h and apoptosis was determined by flow cytometry. (D) Naml6 and SEM cells were treated with indicated concentration of alantolactone and DMSO and then subjected to western blotting assay to detect the cleavage of PARP-1, caspase-3, caspase-8, and caspase-9. (E) Naml6 and SEM cells were treated with alantolactone or DMSO for 12 h and cell cycle was determined by PI staining assay. (F) Naml6 and SEM cells were treated with alantolactone or DMSO for 12 h and subjected to western blotting assay to detect the protein level of ccd2, p-ccd2 (Tyr15), cdc25c, p-cdc25c (Ser216) and β-Actin. Experiments were performed in triplicate.

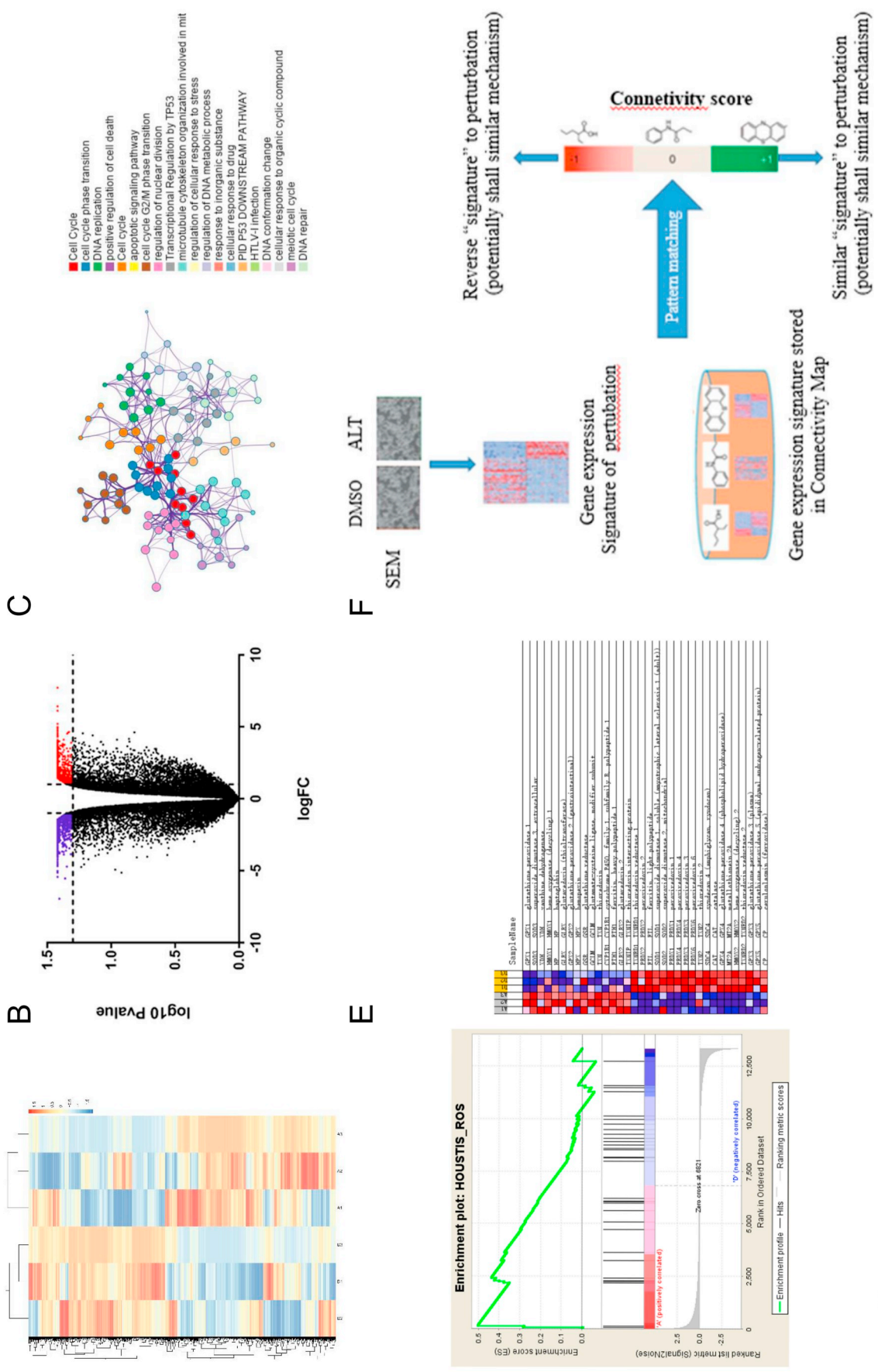

Fig. 3. Bioinformatic prediction demonstrated that Alantolactone exerts its effect may through ROS overload and consequently induced DNA damages. (A) The cluster heat map of expression profiles of mRNA from three alantolactone-treated SEM sample and three DMSO-treated SEM sample. (B) Volcano plot of differential expression genes (DEGs) was drew with R statistical software with a criteria of P value < 0.05 and Fold change (FC) > 2. (C) Enrichment of functions of the DEGs was conducted on metascape platform according to the instruction on the platform. (D, E) Gene set enrichment analysis (GSEA) was performed with GSEA software according to the detailed manual on website. (F) The overall schematic diagram of how the connectivity map works.

Table 2
Top ten drugs shared most similar signature with alantolactone, which was analyzed by connectivity map. Differentially expressed genes list of alantolactone-treated SEM cells were uploaded as a signature to c-Map platform and after matched with the reserved data on the platform, results were returned and ranked according to c-Map score.

Rank	Compound name	Cell line	Mean c-Map score	n	Enrichment	*P* value
1	Parthenolide	MCF7	0.909	2	0.999	< 0.0001
2	Withaferin A	MCF7	0.882	2	1	< 0.0001
3	Celastrol	MCF7	0.85	1	0.999	< 0.0001
4	Phenoxybenzamine	MCF7	0.789	3	0.999	< 0.0001
5	Nedaplatin	MCF7	0.74	1	0.998	< 0.0001
6	Thiostrepton	MCF7	0.728	2	0.998	< 0.0001
7	Lomustine	PC3	0.669	2	0.996	< 0.0001
8	Piperlongumine	MCF7	0.641	1	0.996	< 0.0001
9	Parthenolide	PC3	0.631	1	0.995	< 0.0001
10	Semustine	PC3	0.587	2	0.992	< 0.0001

we have tested if alantolactone could inhibit the activity of enzymes that play important role in elimination of cellular ROS. We have tested the inhibition of alantolacrone on several enzymes including glutathione reductase (GR), thioredoxin reductase (TrxR), catalase and superoxide peroxidase (SOD). Treatment with alantolactone in SEM cells for 12 h obviously inhibited the activity of GR, TrxR and catalase (Fig. 6A) while sparing SOD (Fig. S2A). And similar result were confirmed in Naml6 (Fig. S2B). Then GR and catalase steadily transfected into SEM cells, and confirmed in protein level (Fig. 6D, G). After stable transfection of GR and catalase, the background ROS level was reduced compared with control group (Fig. 6E, H). And overexpression of GR and catalase partially reduce the cells death after treatment with same concentration of alantolactone (Fig. 6F, I). In addition, alantolactone also inhibited the activity of TrxR, which was in coincidence with results previously reported [25]. And overexpression of TrxR in SEM cells induced ROS background level (Fig. S2D) and counteracted the effect of alantolactone (Fig. S2E). In summary, alantolactone inhibited GR, catalase and TrxR activity which partly account for its ROS-inducing effect.

3.8. Alantolactone extended the survival and improves the pathology of B-ALL xenograft mice

In order to test the antitumor effect in vivo, as is shown in Fig. 7A, $1 * 10^7$ SEM cells were injected into NOD/SCID mouse though caudal vein. After seven days, at which time a certain number of mCD45-huCD19+ cells could be detected in peripheral blood, B-ALL model mice were randomly separated into two groups: vehicle group and alantolactone treatment group. In alantolactone treatment group, mice were treated with alantolactone 100 mg/kg by abdominal administration every 2 days and terminated injection after 14 days of treatment, while vehicle group mice were treated with carrier solvent of same volume. Alantolactone significantly extended survival time of mice in alantolactone-treatment group compared with survival time of mice in vehicle-treatment group, as shown with a survival curve analyzed by Kaplan-Meier analysis (Fig. 7B). The average time from diagnosis to death was 23.5 days in the vehicle-treated disease mice (range from 20 to 25 days; n = 6) versus 31.5 days in the mice treated with 100 mg/kg alantolactone (range from 25 to 33 days; n = 6; $P < 0.01$). And weight was documented from the day of receiving therapy to the last day of treatment, and no significant weight loss was observed in alantolactone treatment group compared with vehicle group as is shown in Fig. 6C. On day 21 when mice in vehicle group showed the signs of overt leukemia such as a percentage of human blasts higher than 80% in PB, weight lost higher than 20% and/or hunched posture, mice in both alantolactone treatment group and vehicle group were sacrificed, and bone marrow cells were separated and labelled with human CD19 antibody, flow cytometric analysis showed that alantolactone treatment significantly reduced the number of huCD19-positive leukemia cells in the bone marrow (Fig. 7D). In addition, spleens of mice on twenty-first day in alantolactone group are obviously smaller than vehicle group, as is presented in Fig. 7E, and statistical analysis of spleen weight showed significant difference as is shown in Fig. 7F. And the same time, spleens in both vehicle and alantolactone treatment group were stained with hematoxylin-eosin, and tumor infiltration in alantolactone treatment group are far more less severe than that in vehicle group. These results demonstrated that alantolactone was also effective in vivo.

4. Discussion

In this study, we have confirmed the antitumor efficacy of alantolactone both in vitro in B-ALL cell lines, primary cells from patients and in vivo in B-ALL mice model. And we have demonstrated that alantolactone induced ROS overload and subsequently led to DNA damage, which triggered cell cycle arrest and cell apoptosis. In addition, except inhibition to TrxR [25], alantolactone showed extensive inhibition to enzymes participating in scavenging of cellular ROS to sustain redox homeostasis, such as glutathione reductase (GR), catalase (Fig. 6). And stable transfection of these enzymes partially counteracted the effect of alantolactone (Fig. S2). Besides, we found B-ALL cells including SEM and RS4;11 harboring MLL-AF4 had higher ROS level compared with other no MLL-AF4 infusion B-ALL cells such as Naml6 (Fig. 4B). And SEM and RS4;11 were more sensitive to alantolactone than Naml6 in 24 h treatment (Fig. 4A). And knockdown of MLL-AF4 with siRNAs could significantly reduce the background ROS level in SEM and RS4;11 (Fig. S3D, E). With these results, we may prudently speculate that MLL-AF4 may further enhance cellular ROS level like ras and c-myc oncogene [10,11].

In order to illuminate the mechanism of antitumor effect of alantolactone, a synthetical bio-informatics method has been used and showed relatively good accuracy. Next generation sequencing and volcano plot were used to get differential expression genes (DEGs) and then DEGs was annotated on metascape platform (Fig. 3C). In addition, gene set enrichment analysis (GSEA) was performed to further identify the most related pathway (Fig. 3D, E). What's more, c-MAP platform were used to acquire the possible drugs sharing similar signature, which most likely to share similar mechanism with alantolactone (Fig. 3F). With these synthetical methods, we formed the hypothesis that alantolactone showed anti-cancer effect may through NF-kB inhibition and oxidative stress induced DNA damage (Table 2). This finding is consistent with that of Wei [21] who reported that alantolactone induced apoptosis in chronic myelogenous leukemia through NF-κB inhibition and that of Yushuang Ding who demonstrated that alantolactone prompted oxidative DNA damage and apoptosis in colorectal Cancer Cells [26]. So it could give others some reference in figuring out the underlying mechanism of action of small molecule which remains to be fully illuminated.

Several tumor cell types harboring cytogenetic abnormalities such as BCR-ABL, EGFR, which are critically rely on the sustaining activation of oncogenic pathway essential for their survival, a phenomenon termed “oncogene addiction” [27]. This finding has led to the exploitation of molecular targeted therapeutic drugs, such as tyrosine kinase inhibitors targeting BCR-ABL in chronic myeloid leukemia [28] and EGFR-TKIs targeting EGFR in non-small-cell lung cancer [29,30] and showed extremely effective. Unfortunately, this was frequently followed by the recurrence of drug-resistant tumor clones, which always due to emergency of new mutations on target sites. Recently, it has been reported that the proper function of non-mutated genes enhance the survival of many cancers, a phenomenon called non-oncogene addiction [31]. It is widely reported that cancer cells have relatively higher ROS level compared with normal cells [32]. ROS in tumor cells enhances the tumorigenic phenotype and prompts the accumulation of additional mutations that lead to metastatic behavior [12].

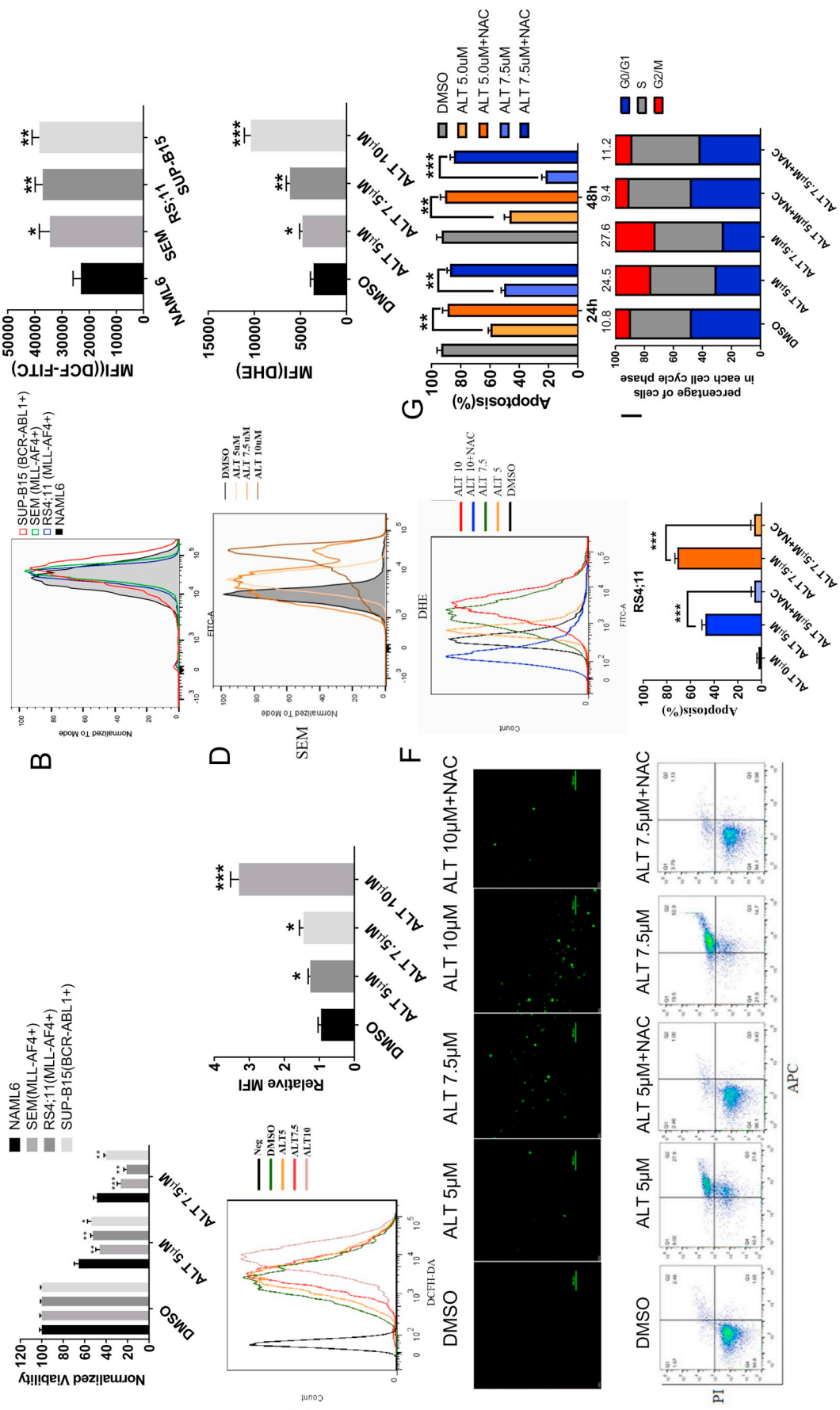

Fig. 4. The antitumor effect of alantolactone is mediated by the overload cellular ROS level. (A) Cell viability of four B-ALL cell lines treated with alantolactone and DMSO was determined by trypan blue assay. (B) The background ROS level of Naml6, SEM, RS4;11 and SUP-B15 was determined by ROS probe DCFH-DA. (C) SEM cells treated with indicated alantolactone and DMSO (0.1%) for 12 h and then ROS level was determined by ROS probe DCFH-DA. (D) SEM cells treated with indicated alantolactone and DMSO (0.1%) for 12 h and then ROS level was determined by ROS probe DHE. (E) SEM cells were treated with indicated alantolactone and DMSO (0.1%) for 12 h or pretreated with NAC (5 mM) for 3 h before treatment with alantolactone. Then cells were incubated with DCFH-DA to assess cellular ROS level with fluorescence microscope. (F) SEM cells treated with indicated alantolactone for 12 h directly or pretreated with NAC (5 mM) for 3 h, and then cells was incubated with DCFH-DA to assess the level of cellular ROS by flow cytometer. (G) SEM cells treated with indicated alantolactone for 24 h and 48 h directly or pretreated with NAC (5 mM) for 3 h, and then cell viability was assessed by trypan blue assay. (H) SEM cells treated with indicated alantolactone for 24 h and 48 h directly or pretreated with NAC (5 mM) for 3 h, and then cell apoptosis was detected by Annexin V-PI staining assay. (I) SEM cells treated with indicated alantolactone for 24 h and 48 h directly or pretreated with NAC (5 mM) for 3 h, and then cell cycle was detected by PI staining assay. Experiments were performed in triplicate ($^{*}P < 0.05$; $^{**}P < 0.01$; $^{***}P < 0.001$).

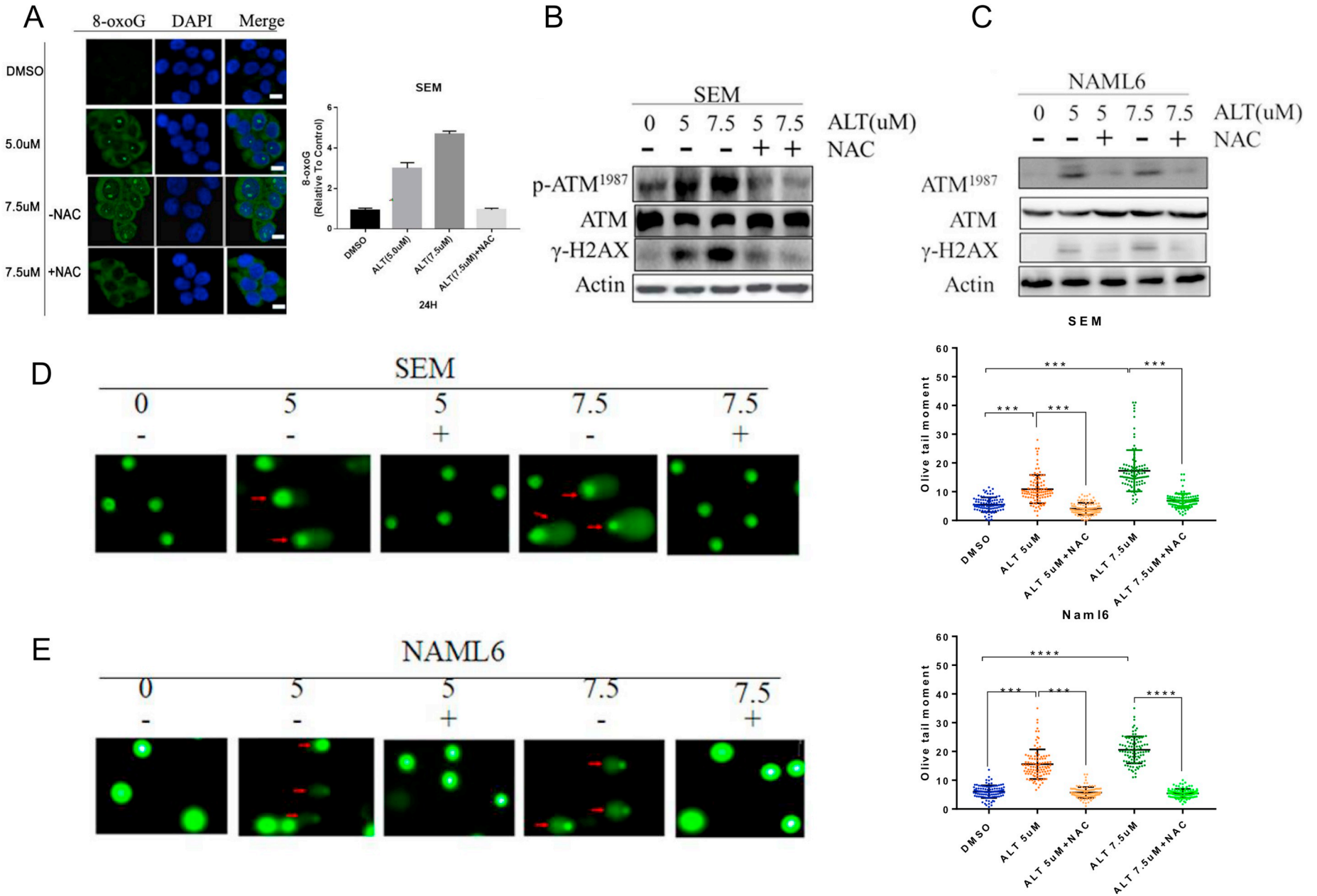

Fig. 5. Alantolactone induced extensive DNA damages in B-ALL cells. (A) SEM cells were treated by alantolactone with or without pretreatment of NAC (5 mM) for 3 h, and 8-oxoG was detected by immunofluorescence and the image quantified by ImageJ software. (B, C) SEM and Naml6 cells were treated by alantolactone for 12 h with or without pretreatment of NAC (5 mM) for 3 h, and then samples were probed with antibodies against ATM, p-ATM^{1987}, γ-H2AX and β-Actin. (D, E) SEM and Naml6 cells were treated with alantolactone for 16 h with or without pretreatment of NAC (5 mM) for 3 h, and then comet assay was used to assess the DNA damage. Olive tail moment of 1000cells was calculated with CASP software. (*$P < 0.05$; **$P < 0.01$; ***$P < 0.001$).

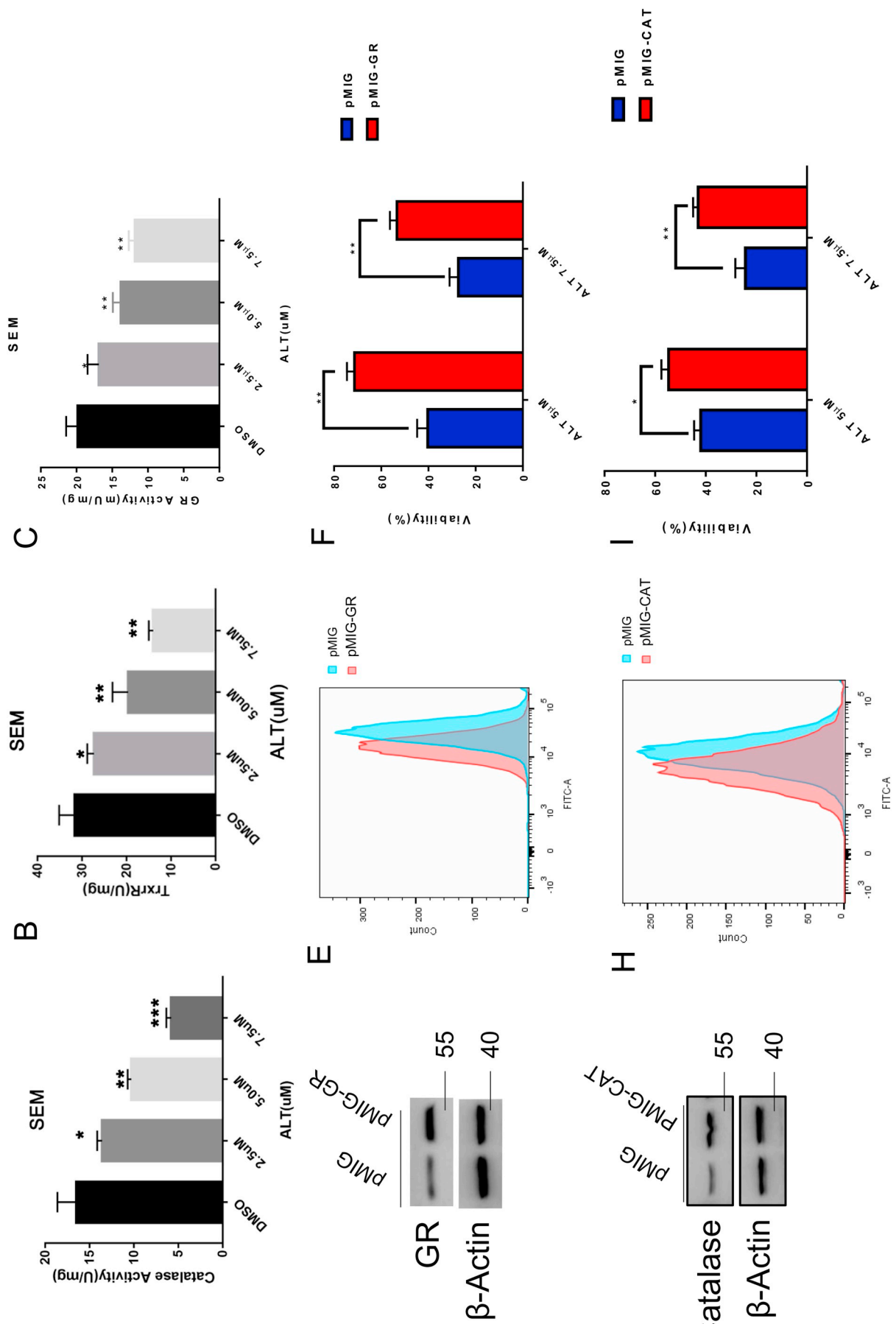

Fig. 6. Alantolactone exerted its effect partly through inhibiting the activity of GR, catalase and TrxR without influencing the activity of SOD. The activity of catalase (A), TrxR (B) and GR (C) were measured after SEM cells treated with alantolactone for 12 h. (D) Expression of protein from SEM cells steadily transfected with GR. (E) SEMs was steadily transfected with GR and then cellular ROS level was measured with DCFH-DA. (F) SEM cells steadily transfected with GR were treated with 5.0 μM and 7.5 μM alantolactone for 48 h and viability was assessed by trypan blue assay. (G) Expression of protein from SEM cells steadily transfected with catalase. (H) SEM cells were steadily transfected with catalase and then cellular ROS level was measured with DCFH-DA. (I) SEM cells steadily transfected with catalase were treated with 5.0 μM and 7.5 μM alantolactone for 48 h and viability was assessed by trypan blue assay.

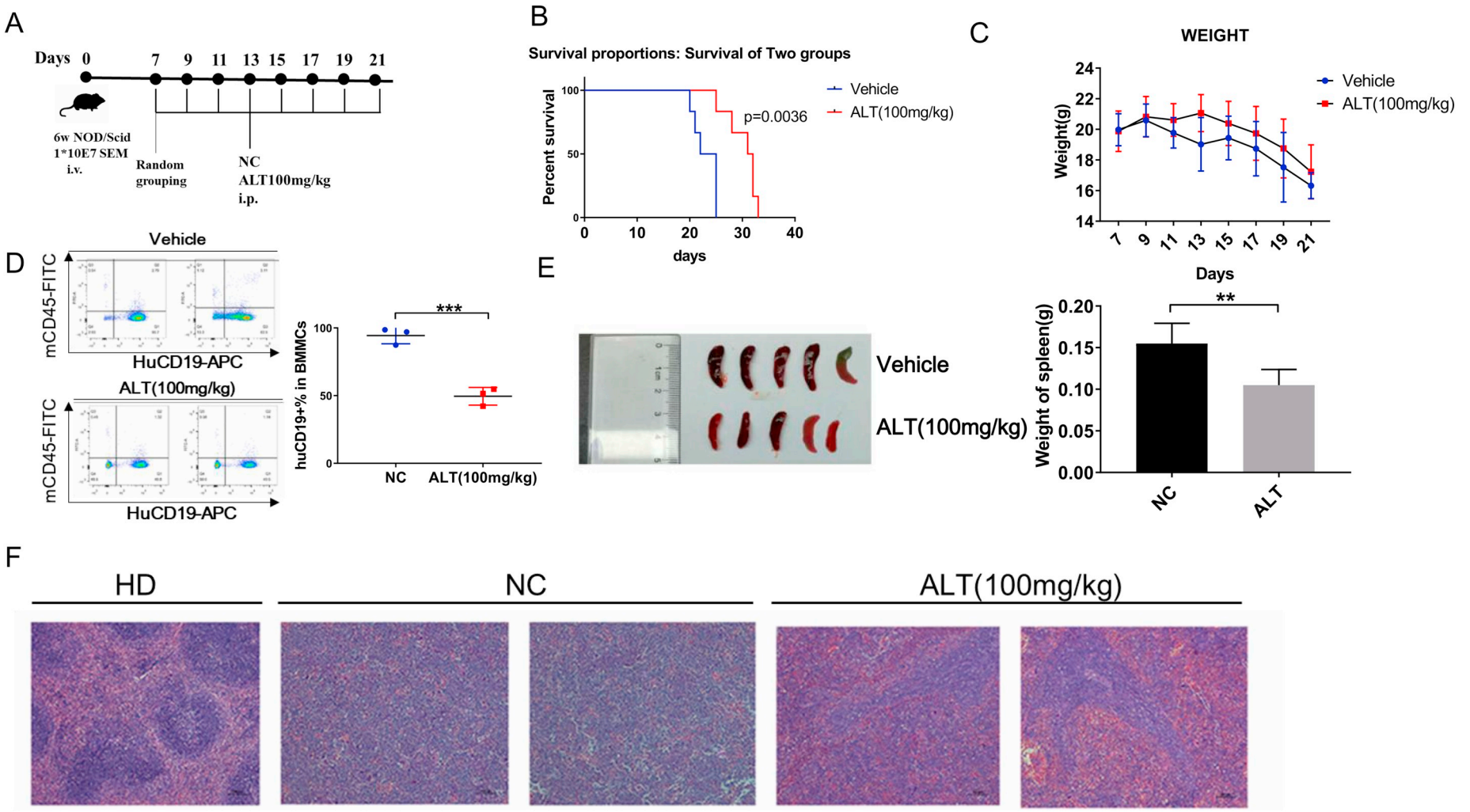

Fig. 7. An in vivo study of the antitumor effect of alantolactone in B-ALL mice model.
(A) A diagrammatic drawing of experimental procedure. (B) Survival curve was drawn with Graphpad7.0 and analyzed by log-rank (Mantel-Cox) test. (C) Weight of mice in each group was documented every two days from the day of mice accepting treatment to the day of ceasing injection. (D) Bone marrow mononuclear cells from mice in alantolactone and vehicle group were stained with huCD19-APC and mCD45-FITC antibodies to analyze the percentage of mCD45- huCD19+ population. (E) Spleens of mice in alantolactone and vehicle group were presented and weight variation in each group was calculated with *t*-test (**$P < 0.01$). (F) Presentation of hematoxylin-eosin staining of spleen from normal mouse and mice in vehicle and alantolactone group.

Adaptation to this stress phenotype is essential for tumor cells to survive, proliferation, and drug resistance and consequently cancer cells may become rely on it that do not generally perform such a vital function in normal cells. Thus this render tumor cells more sensitive to pharmacological ROS insults, which induces oxidant stress–induced cell death, and can be exploited for selective cancer therapy [13,33]. In previous study, a study conducted by professors Schreiber & Sam W. Lee showed good antitumor performance of a ROS inducer piperlongumine [15], and here we also identified the good antitumor effect of alantolactone in B-ALL through inducing cellular ROS generation (Figs. 1, 4). Alantolactone showed extensive inhibition to several hematological malignances (Table 1) and more sensitive in B-ALL cell lines especially in SEM and RS4;11 due to their higher ROS background (Fig. 4A). And in vivo study showed alantolactone significantly prolonged the survival of B-ALL model mice and showed good tolerance. Thus, ROS-inducer alantolactone could be candidate drug in the treatment of B-ALL in the future.

In summary, we have confirmed good antitumor effect of alantolactone both in vitro and in vivo and with bioinformatics methods, we have predicted and proved that alantolactone increased oxidative stress overload through inhibition of antioxidant enzymes and resulted in extensive DNA lesion, which led to cell cycle arrest and apoptosis.

Acknowledgments

This research was supported by the National Basic Research Program of China (973 Program) (NO. 2015CB910403); National Natural Science Foundation of China (81570118 and 8167010683), Shanghai Science and Technology Committee (15401901800 and 16ZR1421400).

Conflict of interest

The authors declare no conflict of interest. None of the contents of this manuscript has been previously published or is under consideration elsewhere. All the authors read and approved the final version of the manuscript prior to submission.

Appendix A. Supplementary data

Supplementary data to this article can be found online at https://doi.org/10.1016/j.lfs.2019.04.034.

References

[1] R. Bassan, D. Hoelzer, Modern therapy of acute lymphoblastic leukemia, J. Clin. Oncol. 29 (5) (2011) 532–543.
[2] M.G.C.G. Hiroto Inaba, Acute lymphoblastic leukaemia, Lancet 381 (2013) 1943–1955.
[3] S.P. Hunger, C.G. Mullighan, Acute lymphoblastic leukemia in children, N. Engl. J. Med. 373 (16) (2015) 1541–1552.
[4] S.P. Hunger, et al., Improved survival for children and adolescents with acute lymphoblastic leukemia between 1990 and 2005: a report from the children's oncology group, J. Clin. Oncol. 30 (14) (2012) 1663–1669.
[5] M. Bardini, et al., Antileukemic efficacy of BET inhibitor in a preclinical mouse model of MLL-AF4(+) infant ALL, Mol. Cancer Ther. 17 (8) (2018) 1705–1716.
[6] S. Lin, et al., Instructive role of MLL-fusion proteins revealed by a model of t(4,11) pro-B acute lymphoblastic leukemia, Cancer Cell 30 (5) (2016) 737–749.
[7] G. Waris, H. Ahsan, Reactive oxygen species: role in the development of cancer and various chronic conditions, J. Carcinog. 5 (2006) 14.
[8] R. Visconti, D. Grieco, New insights on oxidative stress in cancer, Curr. Opin. Drug Discov. Devel. 12 (2) (2009) 240–245.
[9] V. Nogueira, N. Hay, Molecular pathways: reactive oxygen species homeostasis in cancer cells and implications for cancer therapy, Clin. Cancer Res. 19 (16) (2013) 4309–4314.
[10] A.C. Lee, et al., Ras proteins induce senescence by altering the intracellular levels of reactive oxygen species, J. Biol. Chem. 274 (12) (1999) 7936–7940.
[11] O. Vafa, et al., c-Myc can induce DNA damage, increase reactive oxygen species, and mitigate p53 function: a mechanism for oncogene-induced genetic instability, Mol. Cell 9 (5) (2002) 1031–1044.
[12] S.S. Sabharwal, P.T. Schumacker, Mitochondrial ROS in cancer: initiators, amplifiers or an Achilles' heel? Nat. Rev. Cancer 14 (11) (2014) 709–721.
[13] D.G. Deavall, et al., Drug-induced oxidative stress and toxicity, J. Toxicol. 2012 (2012) 1–13.
[14] I.R. Indran, et al., Recent advances in apoptosis, mitochondria and drug resistance in cancer cells, BBA-Bioenergetics 1807 (6) (2011) 735–745.
[15] L. Raj, et al., Selective killing of cancer cells by a small molecule targeting the stress response to ROS (vol 475, pg 231, 2011), Nature 526 (7574) (2015) 596.
[16] Y. Dai, et al., Molecularly targeted radiosensitization of human prostate cancer by modulating inhibitor of apoptosis, Clin. Cancer Res. 14 (23) (2008) 7701–7710.
[17] N. Martinez, et al., The oncogenic fusion protein RUNX1-CBFA2T1 supports proliferation and inhibits senescence in t(8,21)-positive leukaemic cells, BMC Cancer 4 (2004) 44.
[18] M. Thomas, et al., Targeting MLL-AF4 with short interfering RNAs inhibits clonogenicity and engraftment of t(4;11)-positive human leukemic cells, Blood 106 (10) (2005) 3559–3566.
[19] M. Yoo, et al., Exploring the molecular mechanisms of Traditional Chinese Medicine components using gene expression signatures and connectivity map, Comput. Methods Prog. Biomed. (2018).
[20] J. Lamb, The Connectivity Map: a new tool for biomedical research, Nat. Rev. Cancer 7 (1) (2007) 54–60.
[21] W. Wei, et al., Alantolactone induces apoptosis in chronic myelogenous leukemia sensitive or resistant to imatinib through NF-kappaB inhibition and Bcr/Abl protein deletion, Apoptosis 18 (9) (2013) 1060–1070.
[22] M.L. Circu, T.Y. Aw, Reactive oxygen species, cellular redox systems, and apoptosis, Free Radic. Biol. Med. 48 (6) (2010) 749–762.
[23] X. Ba, et al., 8-Oxoguanine DNA glycosylase-1-driven DNA base excision repair: role in asthma pathogenesis, Curr. Opin. Allergy Clin. Immunol. 15 (1) (2015) 89–97.
[24] J. Allgayer, et al., Widespread transcriptional gene inactivation initiated by a repair intermediate of 8-oxoguanine, Nucleic Acids Res. 44 (15) (2016) 7267–7280.
[25] J. Zhang, et al., Inhibition of thioredoxin reductase by alantolactone prompts oxidative stress-mediated apoptosis of HeLa cells, Biochem. Pharmacol. 102 (2016) 34–44.
[26] Y. Ding, et al., Induction of ROS overload by alantolactone prompts oxidative DNA damage and apoptosis in colorectal cancer cells, Int. J. Mol. Sci. 17 (4) (2016) 558.
[27] I.B. Weinstein, Cancer: addiction to oncogenes - the Achilles heal of cancer, Science 297 (5578) (2002) 63–64.
[28] T.P. Hughes, et al., Frequency of major molecular responses to imatinib or interferon alfa plus cytarabine in newly diagnosed chronic myeloid leukemia, N. Engl. J. Med. 349 (15) (2003) 1423–1432.
[29] E.L. Kwak, Anaplastic lymphoma kinase inhibition in non-small-cell lung cancer (vol 363, pg 1693, 2010), N. Engl. J. Med. 364 (6) (2011) 588.
[30] T.J. Lynch, et al., Activating mutations in the epidermal growth factor receptor underlying responsiveness of non-small-cell lung cancer to gefitinib, N. Engl. J. Med. 350 (21) (2004) 2129–2139.
[31] N.L. Solimini, J. Luo, S.J. Elledge, Non-oncogene addiction and the stress phenotype of cancer cells, Cell 130 (6) (2007) 986–988.
[32] L. Tong, et al., Reactive oxygen species in redox cancer therapy, Cancer Lett. 367 (1) (2015) 18–25.
[33] B. Marengo, et al., Redox homeostasis and cellular antioxidant systems: crucial players in Cancer growth and therapy, Oxidative Med. Cell. Longev. 2016 (2016) 6235641.